

1 **Supporting Information**

2 **Behavior of the Chiral Herbicide Imazamox in Soils: Enantiomer**
3 **Composition Differentiates Between Biodegradation and**
4 **Photodegradation**

5 Ignaz J. Buerge,* Roy Kasteel, Astrid Bächli, and Thomas Poiger

6
7 Agroscope, Plant Protection Chemistry, CH-8820 Wädenswil, Switzerland

8
9 *Corresponding author e-mail: ignaz.buerge@agroscope.admin.ch; phone: +41 58 460 6383.

10
11 Number of pages: 6
12 Number of figures: 3
13 Number of tables: 1

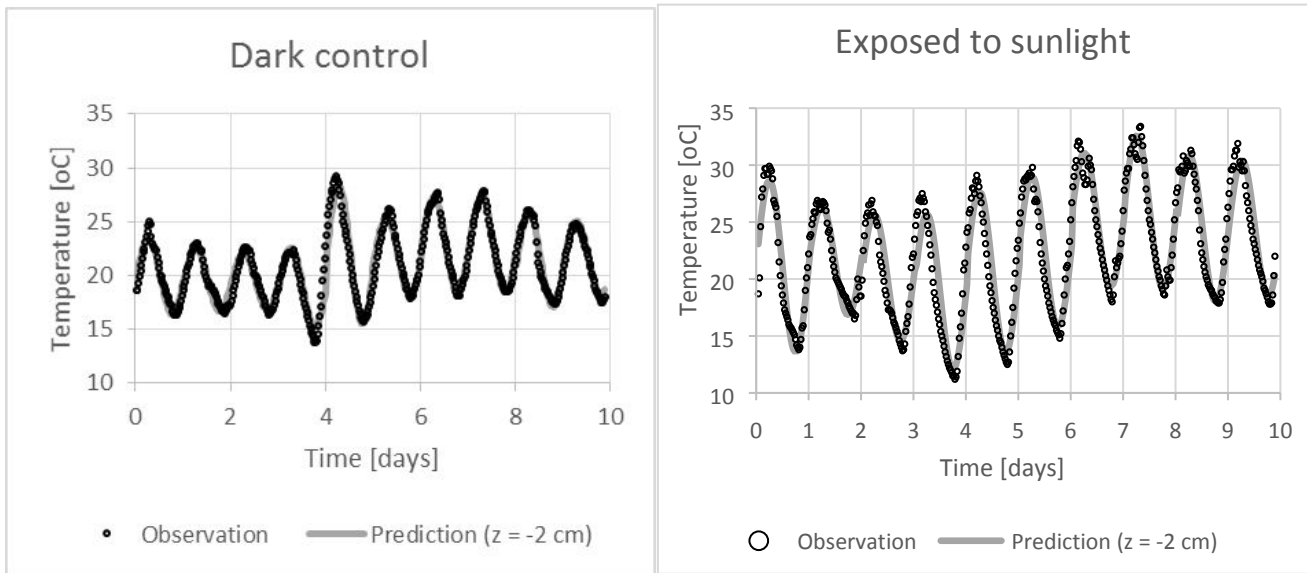
14 Temperature-Dependent Degradation

15 For an assessment of the effect of temperature on the dissipation of imazamox, temperature data were
16 available from two experimental setups, one being exposed to sunlight, the other was a shaded (dark
17 control). The setups were equipped with a temperature logger that was burrowed 2 cm below the soil
18 surface. Temperature was logged at a temporal resolution of 30 min for 10 days (Figure S1).

19

20 Figure S1

21 Daily temperature variations for the dark control and sunlight-exposed dissipation experiments. Symbols
22 are measurements and solid lines model fits.



23

24

25 The solution of the heat flow equation, subject to the upper boundary condition of a periodic wave around
26 an average temperature at the soil surface and to the lower boundary of the average temperature far below
27 the soil surface, is given as follows (Carslaw and Jaeger, 1959):

28

$$29 \quad T(z, t) = T_A + A \exp\left(\frac{z}{d}\right) \sin\left(\omega t + \frac{z}{d}\right) \quad -\infty < z < 0, \quad [\text{Equation S1}]$$

30

31 where T [°C] is the temperature, z [cm] the depth, t the time [d], T_A [°C] the daily average temperature, A
32 [°C] is the amplitude of the temperature fluctuations at the surface, d [cm] is the damping depth, and
33 $\omega=2\pi/\tau$ [d⁻¹] is the angular frequency of the change in temperature at the soil surface, where $\tau = 1$ d is the
34 period of the wave. Although the temperature regime in the clay loam soil was not conform to the solution
35 of the heat flow equation (the soil column was heated up from all sides), Equation S1 was used to describe
36 the effective behavior of the daily temperature variations measured 2 cm below the soil surface. For this,
37 the time series of measured temperatures was split up in waves with a period of 1 day starting at noon.

38 The measured temperatures at 2 cm depth of each particular wave were averaged (T_A) and treated as
 39 constants in the fit. The amplitude A of each wave was fitted, as was the damping depth d , which was
 40 assumed to be the same for the whole period. The actual time was corrected for the time lag, $z/(\omega d)$, to
 41 account for the phase shift of the wave at 2 cm depth with respect to the surface. Figure S1 shows the
 42 adequate fit of Equation S1 to the data and the resulting optimized parameters are summarized in Table
 43 S1.

44
 45 **Table S1**

46 Parameters in the solution of the heat flow equation, describing the measured daily temperature variations
 47 at 2 cm below the surface for the dark control and the sunlight-exposed dissipation experiments.

damping depth d	dark control experiment		sunlight-exposed experiment	
	15.1 cm		3.8×10^5 cm	
day	T_A [°C] fixed from measurements	A [°C] fitted	T_A [°C] fixed from measurements	A [°C] fitted
1	19.9	4.0	21.1	7.6
2	16.6	3.3	21.6	4.8
3	19.5	3.0	20.1	5.6
4	19.0	4.2	18.9	6.8
5	21.9	7.3	20.6	7.1
6	21.8	4.1	22.4	6.6
7	22.8	5.0	25.2	5.9
8	22.9	5.1	25.9	6.8
9	21.5	4.9	24.4	6.4
10	21.6	3.9	24.5	6.0
average (day 1–4)	19.5	3.6	20.4	6.2
average (day 1–10)	21.0	4.5	22.5	6.4

49
 50 As expected, direct exposure to sunlight increased both, the temperature and the amplitude of the
 51 temperature variations, on average by 1.5 and 1.9°C, respectively, for the 10-day period. The increase of
 52 the amplitude was especially large (2.6°C) during the first four days of the dissipation experiments, when
 53 the majority of imazamox dissipated. The physically unrealistic large damping depth for the sunlight-
 54 exposed experiment reflects that heat transfer was very fast, because the soil was heated up (and cooled
 55 down at night) from all sides in absence of any insulation. The consequence is that temperature is identical
 56 at all depths. This effect was not observed in the dark control experiment, because the soil was covered
 57 by a bucket wrapped in aluminum foil.

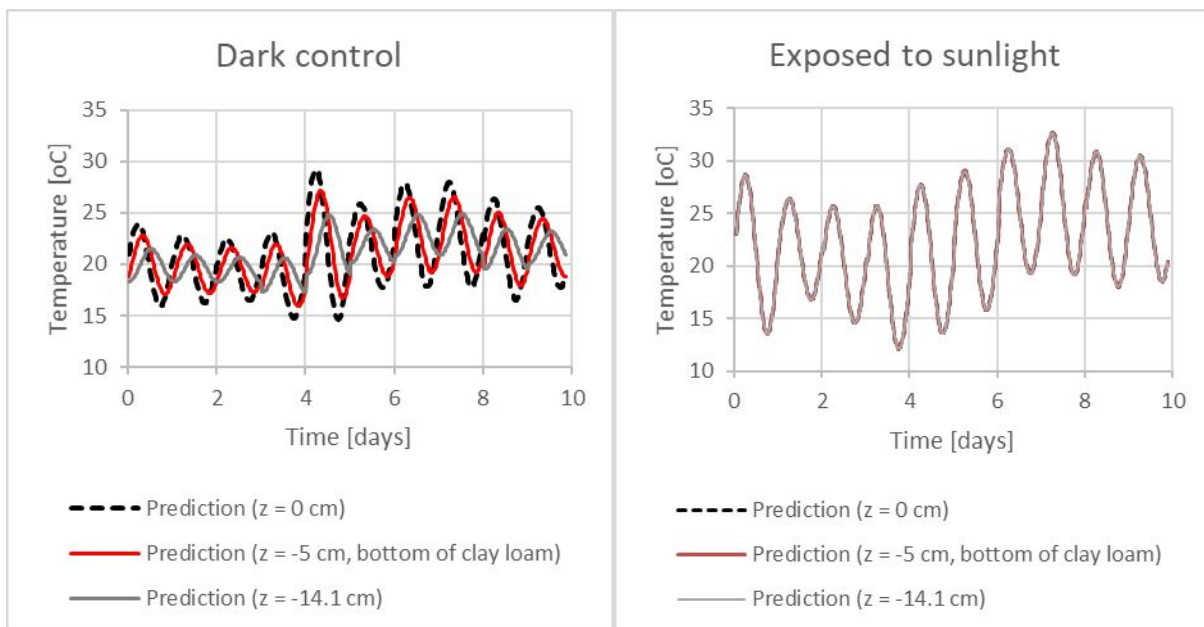
58 The solution of the heat flow equation was extrapolated to the soil surface ($z = 0$), to the bottom of the
 59 soil ($z = -5$ cm), and to the water level ($z = -14.1$ cm), implicitly assuming identical heat properties for
 60 soil and florist foam. The extrapolated values to depths of 0 and -14.1 cm represented the upper and lower

61 boundary condition for temperature, respectively, in the numerical simulations. The results of these
62 extrapolations are given in Figure S2 (extrapolation to $z = +0.3$ cm is not shown as upper boundary for
63 the sand cover).

64

65 **Figure S2**

66 Estimated daily temperature variations for the soil surface ($z = 0$), the bottom of the soil ($z = -5$ cm), and
67 for the water level in the florist foam ($z = -14.1$ cm) for the dark control and sunlight-exposed dissipation
68 experiments.



69

70

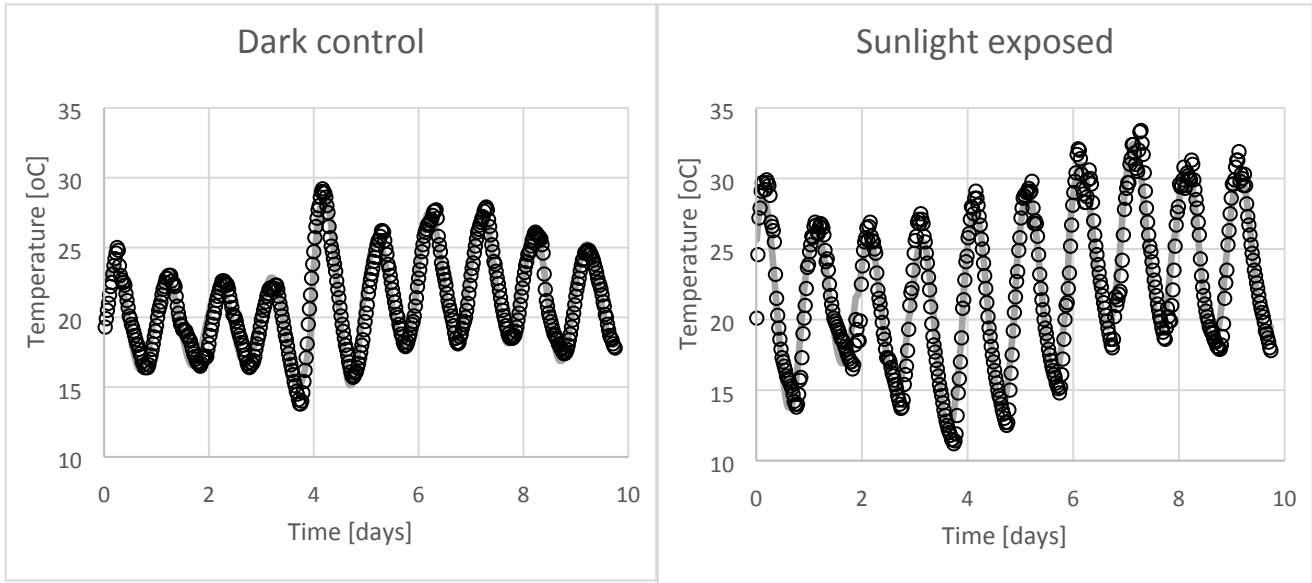
71 Numerical simulations of temperature-dependent dissipation of imazamox were performed with the finite
72 element software package Hydrus-1D version 4.16 (Šimůnek et al, 2013). The calculated temperatures at
73 $z = 0$ ($z = +0.3$ cm for the sand cover) and $z = -14.1$ cm for either the dark control or the sunlight-exposed
74 setup were used as variable upper and lower temperature boundary condition. The heat transport
75 parameters in the temperature module of the package were chosen in such a way that the predicted
76 temperature at 2 cm below the soil surface adequately described the measurements. The volume fraction
77 of the solid phase was set to a value complementary to the saturated volumetric water content (0.55
78 cm^3/cm^3 for the clay loam soil, 0.01 cm^3/cm^3 for the florist foam, and 0.57 cm^3/cm^3 for the sand cover).
79 The longitudinal thermal dispersivity was set either to 5 cm for the dark control or to 1000 cm for the
80 sunlight-exposed setup for all materials (soil, florist foam, and sand cover), which reflects the different
81 thermal regimes observed from the temperature measurements. The thermal conductivity was
82 approximated by the Campbell function which was implemented in the software package. Figure S3 shows

83 the adequate temperature predictions of the numerical model at 2 cm below the soil surface for the dark
 84 controls and the sunlight-exposed setup.

85

86 **Figure S3**

87 Daily temperature variations at 2 cm below the soil surface ($z = -2$ cm) for the dark control and sunlight-
 88 exposed (without sand cover) dissipation experiments. Simulation results (grey line) are compared with
 89 measurements (symbols).



90

91

92 The software package accounts for temperature-dependent degradation rate constants and this temperature
 93 dependency is expressed by the Arrhenius equation as follows:

94

$$95 \quad k_{\text{deg},T} = k_{\text{deg},T_{\text{ref}}} \exp\left(\frac{E_A(T^A - T_{\text{ref}}^A)}{RT^A T_{\text{ref}}^A}\right) \quad [\text{Equation S2}]$$

96

97 where $k_{\text{deg},T}$ and $k_{\text{deg},T_{\text{ref}}}$ [d^{-1}] are rate constants of microbial degradation at the absolute ambient T^A [K]
 98 and the absolute reference temperature T_{ref}^A of 293.15 K (20 °C), respectively, E_A [J mol^{-1}] is the activation
 99 energy, and $R = 8.314 \text{ J K}^{-1} \text{ mol}^{-1}$ is the universal gas constant. The activation energy for microbial
 100 degradation was set to 65400 J mol^{-1} (EFSA 2007).

101 A $k_{\text{deg},T}$ of 0.0245 h^{-1} was determined for the dark control experiments without sand cover at an average
 102 temperature of 19.5°C , measured for the first four days when most dissipation occurred. Using Equation
 103 S2, the rate constant of microbial degradation was 0.0257 h^{-1} at the reference temperature of 20°C . Note
 104 that photochemical degradation and microbial degradation are lumped in an effective rate constant of
 105 dissipation in the numerical model and that photochemical degradation not necessarily follows the same
 106 activation energy as microbial degradation.

107

108 **References**

109 Carslaw, H.S. and J.C. Jaeger, 1959. Conduction of heat in solids. Oxford University Press, London, p
110 510.

111 European Food Safety Authority, EFSA, 2007. Scientific Opinion of the Panel on Plant Protection
112 Products and their Residues on a request from EFSA related to the default Q10 value used to describe
113 the temperature effect on transformation rates of pesticides in soil. The EFSA Journal, 622, 1-32.

114 Šimůnek J, Šejna, M, Saito H, Sakai M, van Genuchten M.T. The HYDRUS-1D software package for
115 simulating the one-dimensional movement of water, heat, and multiple solutes in variably-saturated
116 media, version 4.16; Department of Environmental Sciences, University of California, Riverside: 2013.

117